Model Predictive Control for Reactive Power Management in Transmission Connected Distribution Grids

David Sebastian Stock, Andreas Venzke and Tobias Hennig
Division Energy Economy and Grid Operation
Fraunhofer Institute for Wind Energy and Energy System Technology (IWES)
Kassel, Germany
{sebastian.stock, andreas.venzke, tobias.hennig}@iwes.fraunhofer.de

Lutz Hofmann
Institute of Electric Power Systems
Leibniz Universität Hannover
Hannover, Germany
hofmann@ifes.uni-hannover.de

***Abstract*— In this work a multi-objective model predictive control for reactive power management in transmission connected distribution grids with high share of wind power is presented. The proposed control utilizes reactive power capabilities of wind farms and tap-changer positions in order to improve distribution grid operation. Control signals namely tap-changer positions and reactive power set-points are smoothed over the forecast horizon. Further possible optimization objectives are power loss reduction, voltage profile smoothing and complying with reactive power exchange limits with the transmission grid. A mixed-integer non-linear optimal power flow problem (MINLP-OPF) is formulated incorporating grid operation limits. The performance is evaluated on a real German 110-kV distribution grid with 1.6 GW wind power for one year. With the proposed control, reactive power exchange within allowable limits is increased from 58.3% to 94.5%, compared to a reference operation where only tap-changer positions are utilized for loss reduction with a single time-step optimization.**

***Index Terms*— distributed generation, model predictive control, optimal power flow, reactive power control, wind power grid integration**

I. INTRODUCTION

Over the past decade, growth in renewable generation has led to substantial increase in decentralized generation located in distribution grids [1]. In classical power system operation reactive power has been mainly balanced by large generation units in the transmission grid. In the future, this bulk generation capacity will likely decrease and reactive power provision by distributed generation will gain a significant role [2]. ENTSO-E recently presented the Demand Connection Code (DCC) [3] which defines reactive power exchange limits for transmission connected distribution grids. Maximum allowable reactive power exchange with the transmission grid is set by ENTSO-E at a power factor of 0.9 of either the maximum imported or exported active power. These limits can be further refined by the European transmission system operators. For example, in Switzerland transmission connected distribution grids face payments if the power factor of exchanged power is outside 0.9 inductive to 0.9 capacitive of current imported or exported active power [4]. In Fig. 1 the aforementioned reactive power exchange limits are depicted in a PQ-diagram based on the assumption that maximum exported active power $P_{\mathrm{max,export}}$ is higher than maximum imported active power $P_{\mathrm{max,import}}$.

Several previous works have investigated the reactive power exchange of transmission connected distribution grids. In [5] the reactive power capability of a transmission connected distribution grid for a given active power exchange is assessed. Therefore, the operation of distributed renewable resources is optimized by maximizing the reactive power output of each individual generator. A real-time particle swarm optimization is used in [6] to identify the optimal active and reactive power settings of wind farms to obtain a desired reactive power exchange with the transmission grid. The work in [7] uses model predictive control for active distribution network operation mainly focusing on voltage control. Sensitivity matrices are used for the optimization.

The basic reactive power management strategy used in this work is presented in [8]. This strategy is extended in [9]

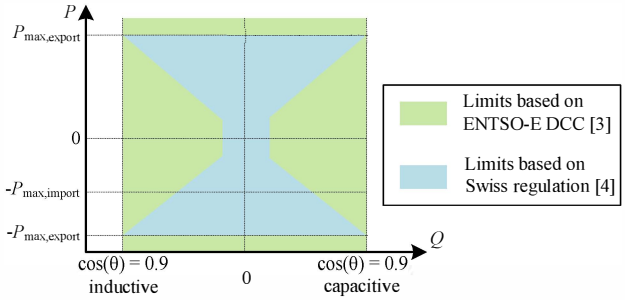

Fig. 1. Limits on reactive power exchange with transmission grid

The presented work is supported by the German Federal Ministry for Economic Affairs and Energy as part of the project "IMOWEN" and the research initiative "Zukunftsfähige Stromnetze".

978-1-5090-5417-6/16/ $ 31.00 ©2016 IEEE

incorporating tap-changer positions and an evaluation of different objective functions. In this work, as novelty to previous works, a multi-objective model predictive control based on a full AC optimal power flow (OPF) is developed which incorporates a forecast of the system. Furthermore, reactive power limits and set-points are included in the OPF formulation. The control variables are smoothed over time in order to avoid excessive tap-changer utilization and frequent changes in control variables which could cause local instability. Overall performance in particular voltage profile and power losses are taken into account as well.

The structure of this work is as follows. In Section II, the utilized methods are explained. The simulation setup is specified in Section III and the obtained results are presented in Section IV. Section V provides the conclusion.

II. METHODS

First, the mixed integer non-linear optimal power flow problem (MINLP-OPF) is stated for a time horizon T. Second, reactive power limits and set-points are included in the formulation with a sequential method. The presented OPF is based on [9] and is extended by forecast horizon, control signal smoothing and reactive power limits. For the modeling, General Algebraic Modeling Language (GAMS) is used [10] and the OPF problem is solved with KNITRO [11].

A. Optimal Power Flow Formulation

The transmission connected distribution grid consists of n nodes. Distribution and transmission grid are connected via grid-coupling transformers. The nodes on the low voltage side of those transformers define the entity M and those on the high voltage side the entity K, respectively. The following objective functions are included in the multi-objective OPF formulation.

$$\min_{u}\left\{\mu_1 f_{\text{profile}} + \mu_2 f_{\text{losses}} + \mu_3 f_{\Delta Q} + \mu_4 f_{Q,\text{gen}} + \mu_5 f_{\text{Tap}}\right\} \quad (2.1)$$

$$f_{\text{profile}} = \sum_{t=1}^{T}\sum_{i=1}^{n}(U_i(t)-U_{\text{S}})^2 \quad (2.2)$$

$$f_{\text{losses}} = \sum_{t=1}^{T}\sum_{i=1}^{n}\sum_{j=1}^{n} G_{ij}(U_i(t)^2 + U_j(t)^2 - \dots \\ 2U_i(t)U_j(t)\cos(\theta_i(t)-\theta_j(t))) \quad (2.3)$$

$$f_{\Delta Q} = \sum_{t=1}^{T}\Big(\sum_{i\in M}\sum_{j\in K} U_i(t)U_j(t) * \dots \\ \left(G_{ij}\sin(\theta_i(t)-\theta_j(t)) - B_{ij}\cos(\theta_i(t)-\theta_j(t))\right) - Q_{\text{set}}\Big)^2 \quad (2.4)$$

$$f_{Q,\text{gen}} = \sum_{t=1}^{T-1}\sum_{i=1}^{n}(Q_{\text{g},i}(t+1)-Q_{\text{g},i}(t))^2 \quad (2.5)$$

$$f_{\text{Tap}} = \sum_{t=1}^{T-1}\sum_{i\in M}\sum_{j\in K}(r_{ij}(t+1)-r_{ij}(t))^2 \quad (2.6)$$

The state variables are the voltage magnitude U_i and angle θ_i for PQ buses, the reactive power $Q_{\text{g},i}$ and voltage angle θ_i for PU buses and the active power $P_{\text{g},i}$ and reactive power $Q_{\text{g},i}$ for Uθ buses. The control variables u are the positions of the transformer tap-changers r_{ij} and reactive power set-points $Q_{\text{g},i}$ of generation units. The transformer tap-changer positions are discrete and modeled with binary variables. G_{ij} and B_{ij} are the branch conductance and susceptance. These are dependent on the actual tap-changer configuration. The following objective functions can be included in the OPF formulation. For voltage profile smoothing, f_{profile} penalizes variation from a voltage set-point U_{s} quadratically. The active power losses in the system are described by f_{losses}. $f_{\Delta Q}$ describes the quadratic deviation from a reactive power exchange set point Q_{set} with the transmission grid. $f_{Q,\text{gen}}$ penalizes variation in the reactive power set-points of generation units quadratically. In addition, variation in tap-changer position is penalized quadratically with f_{Tap}. The factors μ_i denote the objective weights and t the time step. The state and control variables are bounded by the following equality and inequality constraints.

$$\Delta P_i(t) = U_i(t)\sum_{j=1}^{n}U_j(t)G_{ij}\cos(\theta_i(t)-\dots \\ \theta_j(t)) - B_{ij}\sin(\theta_i(t)-\theta_j(t)) = 0 \quad (2.7)$$

$$\Delta Q_i(t) = U_i(t)\sum_{j=1}^{n}U_j(t)(G_{ij}\sin(\theta_i(t)-\dots \\ \theta_j(t)) - B_{ij}\cos(\theta_i(t)-\theta_j(t))) = 0 \quad (2.8)$$

$$Q_{\text{g},i}^{\min}(t) \le Q_{\text{g},i}(t) \le Q_{\text{g},i}^{\max}(t) \quad (2.9)$$

$$U_i^{\min} \le U_i(t) \le U_i^{\max} \quad (2.10)$$

$$r_{ij}^{\min} \le r_{ij}(t) \le r_{ij}^{\max} \quad (2.11)$$

$$-\Delta r_{ij}^{\max} \le r_{ij}(t+1)-r_{ij}(t) \le \Delta r_{ij}^{\max} \quad (2.12)$$

Equality constraints comprise the power balance ΔP_i, ΔQ_i at each node expressed by power flow equations. Inequality resemble the operating limits in particular limitations on reactive generator power injections, restrictions on node voltages U_i and limits of transformer tap changer positions.

B. Consideration of Reactive Power Set-Points and Limits

In the following, a sequential method is outlined to include either a requested reactive power set-point Q_{set} or maximum and minimum reactive power exchange limits $Q_{\text{set,lim}}$, $Q_{\text{set,max}}$. In both cases, the reactive power provision capabilities $Q_{\min}(t)$, $Q_{\max}(t)$ of the transmission connected distribution grid are initially identified by minimizing and maximizing (2.4) with respect to (2.7-2.12). If the requested set-point is outside the calculated limits, it is set to the value of the closest limit. In the next step, the modified set-point $Q_{\text{set}}^{*}(t)$ is introduced as additional equality constraint in the optimization problem.

$$Q_{\min}(t) \le Q_{\text{set}}^{*}(t) \le Q_{\max}(t) \quad (2.13)$$

$$f_{\Delta Q} = \sum_{t=1}^{T} Q_{\text{set}}^{*}(t) \quad (2.14)$$

If reactive power limits are specified it has to be ensured that these are within the feasible reactive power capabilities. These are then included as inequality constraints.

$$Q_{\min}(t) \leq Q^{*}_{\text{set,min}}(t) \leq Q_{\max}(t) \quad (2.15)$$

$$Q_{\min}(t) \leq Q^{*}_{\text{set,max}}(t) \leq Q_{\max}(t) \quad (2.16)$$

$$\sum_{t=1}^{T} Q^{*}_{\text{set,min}}(t) \leq f_{\Delta Q} \leq \sum_{t=1}^{T} Q^{*}_{\text{set,max}}(t) \quad (2.17)$$

III. SIMULATION

A. Grid Modeling

For validation of the proposed control a real German 110-kV distribution grid is examined which is connected to a 220/380-kV transmission grid and several neighboring and underlying distribution grids. A simplified version of the analyzed grid is shown in Fig. 2. The transmission grid is modeled as an external grid with series impedance elements and six buses and is connected via seven grid-coupling tap-changer transformers at three different buses to the analyzed distribution grid. The slack bus is an external grid bus which is not directly connected to the distribution grid.

Generation and loads can be distinguished in three main parts, in particular controllable wind generation, generation and loads in underlying and neighboring distribution grids and remaining uncontrollable wind generation. The distributed generation units in the underlying lower voltage grids are aggregated as single equivalent generator at the corresponding bus. The neighboring 110-kV grids are modeled with external loads at the respective connection nodes. The wind generation and the loads in the examined distribution grid are modeled as PQ buses. In the optimization, only the reactive power of the controllable wind farms can be adjusted. In TABLE 1 the distribution grid characteristics are listed. Maximum exported is significantly larger than maximum imported active power.

TABLE 1. DISTRIBUTION GRID CHARACTERISTICS

Maximum internal/external load (MW)	430/ 500	Number of nodes	167
Maximum total generation (MW)	1640	Number of branches	189
Lower voltage level aggregated generation (MW)	610	Number of transmission grid transformers	7
Controllable wind generation (MW)	525	Remaining wind generation (MW)	505
Total capacitive reactive power exchange (Gvarh)	93	Total inductive reactive power exchange (Gvarh)	241
Maximum imported active power (MW)	600	Maximum exported active power(MW)	1050

B. Reactive Power Modeling

Measurement data from the grid-coupling transformers is available for a complete year. For the modeling, the following assumptions are chosen in order to obtain a similar behavior to the measurements. All generation units in the distribution grid have a power factor of 1.0. The controllable wind generation has an adjustment range from 0.95 inductive to 0.95 capacitive based on regulations in German Grid Codes. The internal and external loads are modeled as having a fixed capacitive reactive power demand and an additional reactive power demand with a power factor which is linearly increasing from 0.98 capacitive to 0.98 inductive with increasing active power demand. Based on these assumptions, the PQ-diagram in Fig. 3 shows measured and simulated reactive power exchange and limits based on ENTSO-E and Swiss regulation. For the Base Case, an optimization is used which only utilizes tap-changer positions to ensure a valid grid operation. During active power import and low active power export, the grid is exchanging significant capacitive reactive power with the transmission grid which is not compliant with the Swiss regulation. With increasing active power export, the exchanged reactive power is becoming increasingly inductive. The significant capacitive contribution is due to cables in the distribution grids and is also reported in research in the UK [12]. For the ENTSO-E limits full compliance is observed for all operating points.

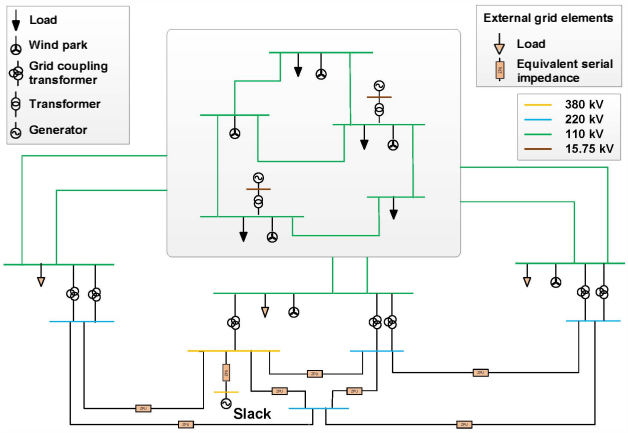

Fig. 2. Simplified representation of transmission connected distribution grid (in green) with external grid

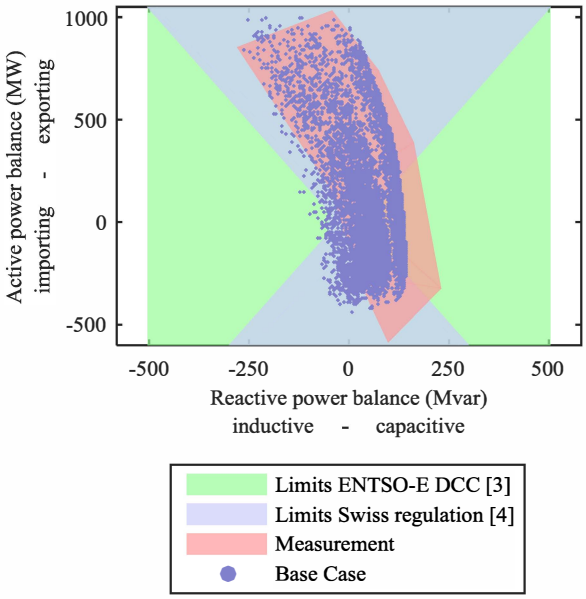

Fig. 3. PQ-Diagram showing reactive power exchange limits and measured and simulated reactive power exchange

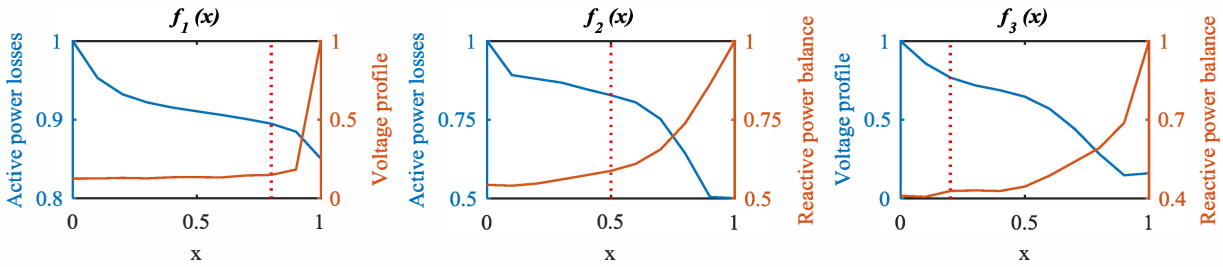

Fig. 4. Trade-off between the objectives loss minimization, voltage profile and neutral reactive power balance where objective values are normalized to 1

IV. Results

First, the trade-off between the different objective weights is assessed in order to identify suitable weights for the multi-objective optimization. Second, the proposed control is evaluated on a real German 110-kV distribution grid with a time series of one year and compared to different single time-step optimizations.

A. Objective Weights

The trade-off between the three different objectives active power losses, voltage profile and reactive power balance is examined. For this purpose, three different simulations are performed with objective functions f_1, f_2 and f_3.

$$\begin{bmatrix} f_1(x) \\ f_2(x) \\ f_3(x) \end{bmatrix} = \begin{bmatrix} x & 1-x & 0 & 0 & 0 \\ x & 0 & 1-x & 0 & 0 \\ 0 & x & 1-x & 0 & 0 \end{bmatrix} \begin{bmatrix} f_{\text{losses}} \\ f_{\text{profile}} \\ f_{\Delta Q} \\ f_{Q,\text{gen}} \\ f_{\text{Tap}} \end{bmatrix} \quad (4.1)$$

The variable x runs from 0 to 1 with a step size of 0.1. The results are evaluated for 150 exemplary time steps and the trade-off graphs are identified by a polynomial fitting and shown in Fig. 4. In the left plot the trade-off between active power losses and quadratic voltage deviation is depicted. If voltage profile is considered with a small weighting factor in the optimization objective, the voltage profile is smoothed substantially and a slight increase in active power losses is observed. For both the graph in the middle and on the right, there is a clear trade-off involved between both objectives. However, again by giving a small weight to loss minimization and voltage profile, the associated performance can be improved with a justifiable increase in reactive power exchange. Based on this, the objective weights μ = [1 0.25 1 1 1] are selected for the multi-objective model predictive control prioritizing neutral reactive power balance and achieving an even trade-off between the remaining objectives. The red dashed lines in Fig. 4 indicate the selected objective weights ratios.

B. Evaluation of Performance

The ability of the proposed model predictive control to obtain a reactive power exchange within allowed limits is evaluated with a time series of one year and compared to different single time-step optimizations. Additional performance criteria are voltage profile, power losses, reactive power set-point profiles and tap-changer operations.

The following simulation configurations are chosen. A time step of 1 hour is used and 2 tap-changer operations per hour are allowed. A voltage bandwidth of 0.9 to 1.1 p.u. is selected. The limits of reactive power exchange for the proposed control are chosen to be +/-100 Mvar which is around 10% of the maximum exported power. This should be seen as a future tight requirement which significantly relieves

TABLE 2. OPTIMIZATION RESULTS TIME SERIES OF ONE YEAR

Control configurations and simulation characteristics	*Base Case*	*Loss Minimization*	*Voltage Profile*	*Neutral Q-Balance (L)*	*Neutral Q-Balance (V)*	*Model Predictive Control*
Objective weights μ	[1 0 0 0 0]	[1 0 0 0 0]	[0 1 0 0 0]	[1 0 0 0 0]	[0 1 0 0 0]	[1 0.25 1 1 1]
Reactive power set-point Q_{set} (Mvar)	--	--	--	0	0	--
Reactive power limits $Q_{\text{set,lim}}/Q_{\text{set,max}}$ (Mvar/Mvar)	--	--	--	--	--	+100/-100
Time horizon T	1	1	1	1	1	4
Absolute reactive power exchange with transmission grid (Gvarh)	718.4	498.0	699.0	277.4	274.6	337.8
Absolute reactive power exchange with transmission grid outside defined limits of +/-100 Mvar (Gvarh)	112.8	43.5	120.1	2.9	2.8	2.4
Quad. deviation from nominal voltage (p.u.)	0.15	0.27	0.03	0.29	0.16	0.14
Active power losses (GWh)	103.7	100.6	117.8	166.7	177.5	161.2
Average tap-changer utilization (%)	13.0	14.5	22.0	30.4	30.0	22.5
Absolute tap changer operations	18749	21217	32749	60096	60071	42234
Average standard deviation reactive power set-points (Mvar)	0	0.66	0.78	0.72	0.80	0.71
Compliance with defined reactive power limits +/-100 Mvar (%)	58.3	76.6	63.0	94.0	93.9	94.5

the transmission grid from the responsibility to compensate reactive power demand from the distribution grid.

For the *Model Predictive Control* a time horizon of 4 time steps is chosen, perfect knowledge is assumed for the forecast and the number of binary variables is reduced from 7 to 4 to decrease computational time. The performance of the *Model Predictive Control* is compared to the following single time-step optimization configurations. For the *Base Case* only the tap changer positions are optimized to minimize losses. *Loss Minimization* and *Voltage Profile* solely minimize the respective objective utilizing tap changer positions and reactive-power capabilities of wind farms. *Neutral Q-Balance (L)* and *Neutral Q-Balance (V)* achieve a neutral reactive power balance if possible and in a second sequential optimization minimize active power losses and voltage profile, respectively.

The detailed parameter configuration and simulation results are shown in TABLE 2. In the analysis, the focus lies on assessing the performance of the *Model Predictive Control*. For a thorough discussion of the single time-step optimization see [9]. Results for *Loss Minimization* and *Voltage Profile* should give an indication for the capability of the optimization to reduce the relevant objective without taking reactive power limitations into account. For the optimizations taking these limitations into account the losses increase as the grid is normally significantly capacitive and by compensation of this capacitive behavior, the voltage level is lowered and losses are increased. The *Model Predictive Control* decreases the absolute reactive power exchange with the transmission grid substantially and achieves with 94.5% the highest level of compliant reactive power exchange. The *Model Predictive Control* uses a multi-objective optimization and not solely focuses on obtaining a neutral reactive power balance. This allows reducing active power losses and smoothing voltage profile in comparison to *Neutral Q-Balance (L)* and *Neutral Q-Balance (V)* by 3.3% and 12.5%, respectively. The benefit of incorporating a forecast is apparent in the reduction in the number of tap operations by 29.7% compared to *Neutral Q-Balance (V)*. The standard deviation of the reactive power set-points is also lowered in comparison to *Neutral Q-Balance (V)*.

In Fig. 5, the PQ-diagram from Fig. 3 is shown with the additional results from the *Model Predictive Control* included. The reactive power exchange is substantially reduced and a compliance of 94.5% with the +/-100 Mvar restriction is achieved compared to an initial compliance of 58.3%. During an import of active power the proposed control is not always able to bring the reactive power balance close to 0 Mvar and remains mainly capacitive. This is due to the fact that wind feed-in is low. However, compliance with the Swiss regulation is also significantly increased.

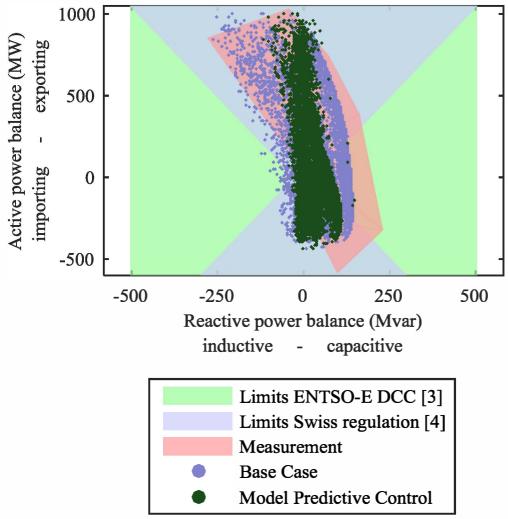

Fig. 5. PQ-Diagram showing reactive power exchange limits and measured and simulated reactive power exchange with Model Predictive Control

V. Conclusion

In this work a multi-objective model predictive control for reactive power management is introduced. An OPF formulation is presented which incorporates a forecast of the system and includes reactive power exchange limits. The proposed control is able to significantly increase compliant reactive power exchange with the transmission grid. In comparison to a single time-step optimization which is minimizing reactive power exchange with the transmission grid, tap changer operations are decreased by 29.7% while performance regarding power losses and voltage profile is improved. In future work, the effect of forecast uncertainty on the controller performance is examined.

References

[1] T. Ackermann, G. Andersson, and L. Söder, "Distributed generation: a definition," *Electric power systems research*, vol. 57, no. 3, pp. 195–204, 2001.

[2] A. Keane *et al*, "State-of-the-art techniques and challenges ahead for distributed generation planning and optimization," *IEEE Transactions on Power Systems*, vol. 28, no. 2, pp. 1493–1502, 2013.

[3] ENTSO-E, "Network Code on Demand Connection," 2012.

[4] M. Kurzidem, "Voltage support concept for the Swiss transmission system from 2011," 2011.

[5] P. Cuffe, P. Smith, and A. Keane, "Capability chart for distributed reactive power resources," *IEEE Transactions on Power Systems*, vol. 29, no. 1, pp. 15–22, 2014.

[6] R.I. Cabadag, U. Schmidt, and P. Schegner, *Reactive power capability of a sub-transmission grid using real-time embedded particle swarm optimization*: IEEE PES Innovative Smart Grid Technologies 2014, Europe, 2014.

[7] G. Valverde and T. van Cutsem, "Model predictive control of voltages in active distribution networks," *IEEE Transactions on Smart Grid*, vol. 4, no. 4, pp. 2152–2161, 2013.

[8] S. Stock and L. Hofmann, "Moderne Optimierungsverfahren zum Betrieb von Windparkclustern in Norddeutschland," *EnInnov2016 - 14. Symposium Energieinnovation*, Graz, 2016.

[9] S. Stock, A. Venzke, L. Löwer, K. Rohrig, and L. Hofmann, "Optimal Reactive Power Management for Transmission Connected Distribution Grid with Wind Farms," in Submission, 2016.

[10] GAMS Development Corporation, *General Algebraic Modeling System (GAMS) Release 24.6*. Washington, DC, USA. Available: http://www.gams.com/.

[11] R. H. Byrd, J. Nocedal, and R. A. Waltz, "KNITRO: An integrated package for nonlinear optimization," in *Large-scale nonlinear optimization*: Springer, 2006, pp. 35–59.

[12] C.G. Kaloudas, L.F. Ochoa, I. Fletcher, B. Marshall, and S. Majithia, Eds, *Investigating the declining reactive power demand of UK distribution networks*: 2015 IEEE Power & Energy Society General Meeting, 2015.